Simulation of PD RF Propagation in MV Bus Bar Chambers

Mijodrag Miljanovic[1], Martin Kearns[2], Brian G Stewart[1]

[1]The Institute of Energy and Environment, University of Strathclyde, Glasgow, Scotland, UK

[2]EDF Energy, Glasgow, Scotland, UK

***Abstract*- The monitoring of partial discharge (PD) in air-insulated medium voltage (MV) switchgear can reveal potential insulation failure. In particular, the application of non-intrusive methods such as radio frequency (RF) sensors may be employed to establish continuous PD level tracking. However, there is still clarification needed to understand the most effective placement of RF probes, especially along extended MV switchgear compartments. Therefore, the aim of the current work is to investigate PD RF signal propagation and signal energy sensitivity along three aligned arbitrary MV switchgear bus bar compartments. A particular model was created by applying finite element methods (FEM) and a grid of probes is created along the chamber structures. By using calculation methods and creating interpolation maps, the potential higher measurement sensitivity regions can be revealed for different PD source locations.**

Keywords- switchgear insulation; partial discharge, EM wave propagation; finite element method (FEM); bus bar compartment

I. INTRODUCTION

Medium voltage (MV) switchgear is a primary component within the electrical grid infrastructure. In addition, insulation failures in switchgear are responsible for more than 40% of outages [1]. The estimation of insulation condition during regular inspections is a focus of maintenance work so as to avoid unexpected interruptions. Since PD activity level might be a good forecast for insulation degradation, there are different techniques that can be applied. One of the commonly applied PD detection techniques on MV switchgear is on-line radio frequency interference (RFI) monitoring as it is fundamentally a non-intrusive method [2].

There are many approaches and suggestions for setting up the sensors around a single MV switchgear cubicle for efficient PD monitoring. In [3] an investigation was performed by placing UHF sensors in switchgear compartments. Based on an attenuation principle the potential fault in a particular compartment may be pinpointed. In [4] an experimental study of UHF sensor applications on single MV switchgear was performed with the propagation and signal characteristics studied depending on artificial insulation defects.

While studying PD detection and the optimum sensor positions in different switchgear compartments, the bus bar compartment turned out to be the most challenging due to its inaccessibility and lack of direct line of sight [5]. PD detection in MV bus bar compartments is also especially of interest for the case of multiple connected switchgear compartments. In [1] it was also reported that transitions from one bus bar compartment to another is prone to higher PD occurrences and insulation defects. In addition, the sensitivity of RF sensors suffers when placed on the outside surface of the compartment due to the metallic encapsulation [6].

To increase RFI signal sensitivity, it is preferable to attach the sensors within the bus bar compartment. But when doing this, particular switchgear or even neighboring units need to be taken out of operation. To avoid placing sensors based on trial and error and additional system outages for corrections it is of value to know in advance where potential or optimum RFI locations exist. Therefore, in this work a potential best evaluation position for sensor location is studied based on calculated signal energy and created interpolation maps along compartment surface walls. The paper is structured as follows. In section II the creation of the simulation model is explained. In section III results are presented and in section IV conclusions are drawn.

II. SIMULATION MODEL

A. Model and Simulation

Finite element method (FEM) simulations are conducted using Comsol Multiphysics. Three bus bar compartment models from an arbitrary switchgear are created. Each model includes supports made of epoxy resign and double bare bus bar conductors with a cross section of 10 x 85 mm². The compartment cage is modelled as 3 mm steel walls.

A triple bus bar line up structure is created, as seen in Fig. 1. Forty-nine COMSOL measurement probes are distributed along the inner surfaces of the compartment walls and associated boundary conditions applied. The surfaces of the conductors and the surface walls are set up as perfect electric conductors. For the simulation the PARDISO solver with Generalized-alpha time-stepping is used; a common solver for electromagnetic (EM) wave propagation simulations. The simulation time step is set to 1 ps and the output time of results to 0.1 ns. The duration of the simulation is set to 25 ns.

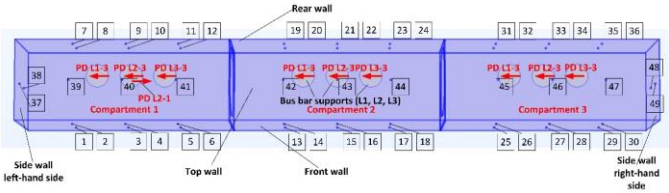

Fig. 1. 3 bus bar line-up compartment model with attached sensors along compartment surfaces and PD sources within compartment

This is a peer-reviewed, version of record of the following paper: Miljanovic, M., Kearns, M., & Stewart, B. G. (2023). Simulation of PD RF propagation in MV bus bar chambers. 1-4. Paper presented at 98th IEEE Conference on Electrical Insulation and Dielectric Phenomena, East Rutherford, New Jersey, United States.

B. PD Source

The PD source is applied separately on each bus bar support along the compartments, as indicated in Fig. 1 by red arrows. The PD source at each support in the FEM environment is represented by a lumped port in the form of a square of 10 mm by 10 mm dimensions. It is placed at the transition spot between the insulation, bus bar conductor and air, as shown in Fig. 2. The current density ($\boldsymbol{J}_s$) is taking place along the surface between the terminals of the lumped port in the positive z-direction, by setting the current parameter in Comsol, $a_{h,z}$ to 1. The implemented PD pulse is based on the Gaussian pulse function according to Eq. (1), as stated in [7].

$$i_{PD}(t) = I_0 * e^{-\left[\frac{(t-t1)^2}{2*\tau^2}\right]} \qquad (1)$$

By changing the parameter τ different pulse widths can be achieved. For the current simulation the value was set to 0.127 ns to create a narrow pulse width. The peak current (I_0) is set to 1A and the term t_1 set to 5 ns, which is the time when the peak of the PD pulse occurs after starting the simulation.

C. Investigation Procedure

The PD pulse generates an EM wave which propagates within the compartment. The induced electric fields normal to the particular plane wall are recorded by the RF probes and stored in csv-files. Within Matlab, a procedure was created which applies the linear interpolant function to create the signal energy maps based on the recorded data according to Eq. (2).

$$E_{signal} = \sum_0^N |x[n]|^2 \qquad (2)$$

In Eq. (2) E_{signal} stands for accumulated signal energy and $x[n]$ are the particular time samples of the signal, which absolute values are squared and taken into a summation function from the first (0) to the last sample (N). A 3-D surface geometry (stl-file) is created in Comsol and imported into Matlab. The generated interpolation maps for each compartment wall are overlayed on the particular surfaces and represented as an interpolation figure map in Matlab.

III. Simulation Results

A. In general

The orientation of the PD source at the particular support may be in 4 different directions. In this simulation the PD of LX-3 was applied, where X stands for the particular phase (L1, L2 or L3) and where the index 3 stands for the direction "to the left-hand side", which is indicated in Fig. 1 by arrows. For the case here simulations are performed for orientation PD LX-3 at each support in different compartments C1, C2, C3. In the first step the signal energy is calculated for each of the probe position along the compartments C1, C2 and C3. The highest signal energy positions detected for each PD source in different compartment positions are shown in Table I.

The slightly darker marked cells represent the highest calculated signal energy of the particular compartment where PD occurs. The brighter cells in the same column represent the highest detected signal energy position in the neighboring compartment. For example, when looking at PDL1-3 in compartment 1 (C1) probe position P7 has the highest signal energy of 115 nJ, whereas for the same PD source position P19 and P31 detect the highest signal energy in other compartments. Generally, the highest signal energy appears for the case of PDL1-3 in compartment 2 (C2) at P19 with 1790 nJ.

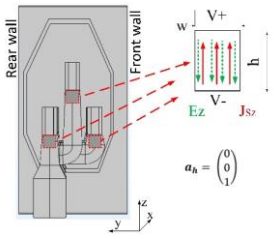

Fig. 2. PD source represented by so-called lumped ports at each phase

In addition to the above by looking at Table I, it can be recognized that for PD sources PDL1-3 and PDL3-3 in different compartments there is some kind of symmetry where the highest signal energy positions occur. For PDL1-3 the symmetry is completely matched since for each compartment the highest signal energy is detected at the same location. For PDL3-3 the symmetry is broken as the PD source is in compartment 3 with probe detection in compartment 1. For PDL2-3 there is higher asymmetry as it can be seen when comparing PD detection in C1 and C2 for PD locations in compartments 1 (C1) and 2 (C2). It seems that the position of the support within the compartment has a significant influence on detection symmetry, since support L2 is placed in the middle of each compartment compared to the other two supports.

TABLE I. Highest Signal Energy Detected (in Nano Joules nJ) for PD on Different Supports in Different Compartments

		PDL1-3			PDL2-3			PDL3-3		
		(C1)	(C2)	(C3)	(C1)	(C2)	(C3)	(C1)	(C2)	(C3)
C1	P3	9.43	6.72	1.70	3.24	3.2	1.1	448	4.9	1.3
	P7	115	10.4	2.06	2.49	2.8	1.3	23.8	3.5	1.4
	P10	9.75	6.55	1.80	9.65	2.1	1.1	16.1	3.9	0.8
C2	P15	3.17	5.99	4.97	6.68	4.1	2.9	31.4	45.4	4.9
	P16	3.20	6.64	4.41	0.507	8.6	3.1	12.6	18.5	3.4
	P19	5.88	1790	6.48	0.8	5.4	2.0	18.5	9.1	2.9
C3	P27	2.30	2.24	5.47	0.5	1.2	4.7	23.7	3.3	35.1
	P28	1.67	1.10	5.33	0.33	7.7	10	7.6	1.6	15.4
	P31	3.31	3.59	665	0.4	1.3	5.4	12.6	3.2	11.1

B. PD on phase L1 in different compartment

In the following, the interpolation maps are described and the time plots are shown for PD on phase L1 in different compartments. As an example, in Fig. 3 the interpolation map is presented for the case of PDL1-3 in compartment 2 (C2). The highest signal energy location is marked by an asterisk at position P19 on the rear wall of the compartment.

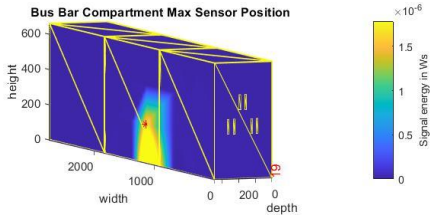

Fig. 3. Interpolation map for PDL1-3 in compartment 2 showing P19 with highest detected signal energy

For this PD case the highest signal energy probe position detected can also be confirmed by looking at Table I. It can be seen that the higher signal energy region appears at the bottom edge of compartment 2. This makes sense, due to the proximity of the particular bus bar support to the probe position.

For the simulations of PD sources on phase L1 in compartments 1 (C1) and 3 (C3) nearly the same maximum signal energy locations are occurring, with reference to the particular compartment. Form Table I these positions are P7 for PDL1-3 in (C1) and P31 for PDL1-3 in (C3). Comparing these positions with Fig. 1 it can be seen they are on the same sides of the wall. In addition, the signal energy interpolation maps appear similar in pattern at the bottom edge of the particular compartment where the PD takes place, as also shown in Fig. 3. Therefore, to avoid repeating similar figures, the case of PD on L1 in compartment 2 was chosen as a representative example for compartment 1 and 3.

In Fig. 4 the normalized electric field - time plots are shown for all maximum signal positions along the three compartments, where the highest energy was detected for the case of PD source on phase L1-3 in different compartments. The probe positions P7, P19 and P31 have the highest signal amplitudes, in case PD location is in the particular compartment. All of these probe positions are at the rear side of the compartment, which is due to the proximity of the PD source to the particular wall. It can be also noticed that the peaks of those signals occur around 0.5 ns after the PD peak takes place, which corresponds to a propagation distance to the wall of 150 cm, with EM wave propagation speed of 0.3 m/ns.

From the time plots, the detected signal P19 for PDL1-3 in compartment 2 possesses the highest amplitude and due to that, also the highest signal energy according to Table I. Comparing the signals in other compartments, it can be seen their peaks are considerably lower in comparison to when PD occurs in the same compartment. In addition, the first peaks of signals in neighbouring compartment appear around 3 to 7 ns after the PD takes place due to the distance from the PD source to the particular sensor in the neighbouring compartment.

C. PD on phase L2 in different compartment

For probe positions in compartment C1 for PDL2-3 in different compartments, it can be seen from Table. I that there is no particular symmetry for the positions where the highest energy has been detected compared to e.g. for PD source on L1. This condition can be also recognized in the interpolation maps in Fig. 5 and Fig. 6. For PDL2-3 in compartment 2, Fig. 5(a), and compartment 3, Fig. 5(b), the position of highest signal energy is at the same front wall of the structure, though there is a slight difference in the interpolation map patterns. Comparing the occurrences of the highest signal energy locations for PDL2-3 in compartment 1 (C1) in Fig. 6(a), despite the similar interpolation map patterns it can be seen that the highest signal energy area has changed to the compartment rear wall side. However, for the case of PDL2-1 in compartment (C1), which is the PD source in the opposite direction to PDL2-3 at the same support, it can be seen from Fig. 6(b) that the pattern is on the same side of the compartment as for PDL2-3 in C2, Fig. 5(a),

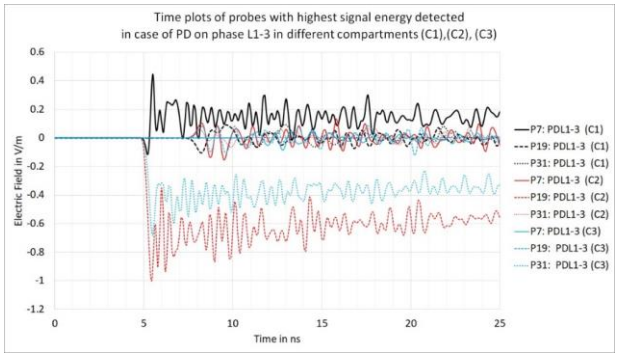

Fig. 4. Normalized electric field time plots of probes with highest amplitudes detected in case of PD on L1-3 in different compartments.

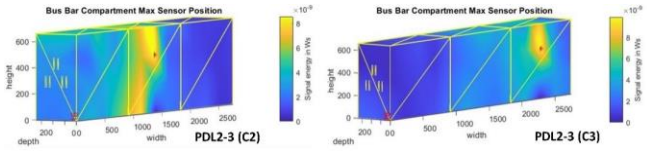

(a) PDL2-3 in C2 (b) PDL2-3 in C3

Fig. 5 Front wall view of interpolation maps in case of PDL2.3 in C2 and PDL2-3 in C3.

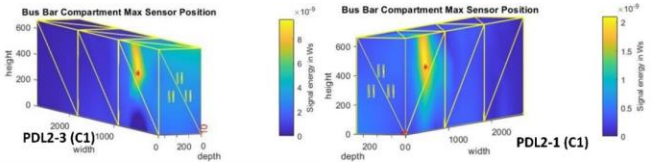

(a) PDL2-3 (C1) (b) PDL2-1 (C1)

Fig. 6. Rear wall view of interpolation maps in case of PDL2-1 in C1 and L2-3 in C3.

and for PDL2-3 in C3, Fig. 5(b). The occurring asymmetry seems to be due to the orientation of the PD source within the compartment and the position of the bus bar support. For PDL2-3 in C3, Fig. 5(b) and PDL2-1 in C1, Fig. 6(b), the orientation of the PD sources are in the opposite directions in reference from the particular neighboring side wall. This is also visible from Fig. 1 when comparting the arrows of L2-1 in C1 and L2-3 in C3, which are orientated to each other and showing away from the particular side wall.

In Fig. 7 the electric field - time plots of the positions with the highest signal energy detected for each compartment for PD source PDL2-3 are presented. The detected signals for P10, P16 and P28 possess the highest amplitudes in case PD is in the compartment of the particular probe.

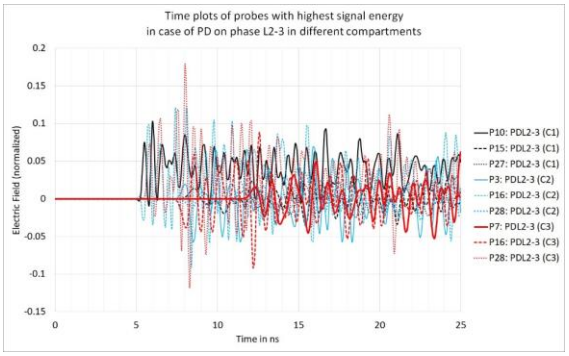

Fig. 7. Normalized electric field time plots of probes with highest amplitudes detected in case of PD on L2-3 in different compartments.

This is due to the fact that these probe positions are very close to the particular PD source for this situation, as can also be seen from Fig. 1. Comparing the probes in Fig. 4 for the case of PD on L1, it can be seen that the signal amplitudes are generally a bit lower. This is likely due to the middle position of the particular support in the compartment and therefore the available space is not limited for the EM wave to propagate in both directions comparing to the other two supports. In addition, it can be also recognized that for example the first peak of the probe P7 appears around 7 ns in delay after PD takes place. This corresponds to the distance of around 2 m from the PD source to the particular probe position.

D. PD on phase L3 in different compartments

In Fig. 8 the energy interpolation map is shown for PDL3-3 in compartment 2. The highest signal energy location appears at the front wall of the compartment at position P15 due to the vicinity of the bus bar support to the particular wall. The interpolation maps for PDL3-3 in compartment 1 and PDL3-3 in compartment 3 also form similar patterns but with different highest energy probe positions. For PDL3-3 in compartment C1, the highest signal energy appears at P3, whereas for PDL3 in C3 it is probe P27. However, all of the positions with highest signal energy appear on the front wall of the structure. Comparing with PD on phase L2 in the previous case, it can be seen that a higher signal energy pattern tends to occur at the left bottom edge part of the compartment. This is due to the shorter distance and the size of the particular support to the wall.

In Fig. 9 the electric field - time plots are shown for PDL3-3 in different compartments. It can be seen that the amplitudes for positions P3, P15 and P27 possess the highest values when the PD source occurs in the particular compartment. Interestingly the amplitude at position P15 for PDL3-3 in C1 is also very high along with P3 compared to other signals. This might be due to the reflection characteristics of the EM wave within the compartment. Comparing all the three time-plots form Figs. 9, 7 and 4 together, it can be noticed that the signals with the highest amplitudes tend to appear mainly either in the positive or negative half of the plot. The other signals, which probes are further away from the particular PD source, are oscillating mainly around the zero axis. It was found out that in case of further reducing the PD pulse, the oscillation of these signals would also move to the zero axis, which seems to be due to the wave length of the generated EM wave by the particular PD source.

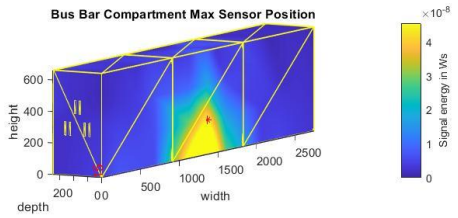

Fig. 8. Interpolation map for PDL3-3 in compartment 2 with P15 showing the highest signal energy detected

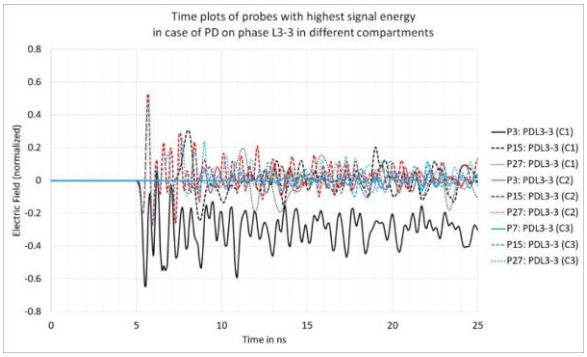

Fig. 9. Normalized electric field time plots of probes with highest amplitudes in case of PD on L3-3 in different compartments.

IV. CONCLUSIONS

By applying signal energy interpolation maps it can be seen that optimum PD sensor location patterns change depending on the position of PD sources along a three compartment bus bar structure. However, it has been shown that the highest signal energy areas can be visualized through these maps, which will provide assistance for optimum senor position placement and more efficient PD detection. For all the PD sources the front and rear wall seems to be applicable for PD detection, while side walls do not represent an optimum place for sensor positions.

It has been also shown that the position of the potential higher sensor sensitivity depends on where the PD occurs on the bus bar supports. In addition to that, the patterns of higher signal energy show some kind of pattern regularity or similarity for the two outer supports in a compartment comparing the interpolation maps patterns for the middle-placed bus bar supports from phase L2.

ACKNOWLEDGMENT

This work was funded by EDF (UK).

REFERENCES

[1] G. Paoletti and M. Baier, Failure contributors of MV electrical equipment and condition assessment program development, *Conference Record of 2001 Annual Pulp and Paper Industry Technical Conference (Cat. No.01CH37209)*, Portland, OR, USA, 2001.

[2] A. Nesbitt, B. G. Stewart, S. G. McMeekin, K. Liebech-Lien and H. O. Kristiansen, "Substation surveillance using RFI and complementary EMI detection techniques," *PES T&D 2012*, Orlando, FL, USA, 2012

[3] C. Pestell, S. Broderick and D. Caves, "Identification and location of partial discharge in medium voltage switchgear using radio frequency detection techniques," *2017 Petroleum and Chemical Industry Conference Europe (PCIC Europe)*, Vienna, Austria, 2017.

[4] Liuhuo Wang *et al*., "Experimental investigation of partial discharge detection in medium-voltage switchgear based on Ultra-High-Frequency sensor," *2013 2nd International Conference on Electric Power Equipment - Switching Technology (ICEPE-ST)*, Matsue, 2013.

[5] J. E. Smith, G. Paoletti and I. Blokhintsev, "Experience with on-line partial discharge analysis as a tool for predictive maintenance for medium voltage (MV) switchgear systems," *Record of Conference Papers. Industry Applications Society. Forty-Ninth Annual Conference. 2002 Petroleum and Chemical Industry Technical Conference*, New Orleans, LA, USA, 2002.

[6] L. J. Wang *et al*., "Experimental investigation of typical partial discharge signals in medium-voltage switchgear," *2014 International Symposium on Discharges and Electrical Insulation in Vacuum (ISDEIV)*, Mumbai, India, 2014.

[7] M. D. Judd, O. Farish and B. F. Hampton, "The excitation of UHF signals by partial discharges in GIS," in *IEEE Transactions on Dielectrics and Electrical Insulation*, vol. 3, no. 2, pp. 213-228, April 1996.